







MODEL OF RADIATION-INDUCED MOTION OF LIQUID INCLUSIONS IN CRYSTAL[†]

 Oleksandr P. Kulyk^{a*},  Oksana V. Podshyvalova^b,  Mykhailo Yu. Shevchenko^{a,c},
 Victor I. Tkachenko^{a,c,†},  Iryna V. Hariachevska^a,  Toru Aoki^d

^aV.N. Karazin Kharkiv National University, 4 Svobody Sq., Kharkiv 61022, Ukraine

^bNational Aerospace University "Kharkiv Aviation Institute", 17 Chkalov St., Kharkiv 61070, Ukraine

^cNational Science Center "Kharkiv Institute of Physics and Technology", 1 Akademichna St., Kharkiv 61108, Ukraine

^dResearch Institute of Electronics, Shizuoka University, 3-5-1 Johoku, Naka-ku, Hamamatsu 432-8011, Japan

*Corresponding author e-mail: kulykop@gmail.com

[†]E-mail: tkachenko.vikiv52@gmail.com

Received July 10; revised August 19, 2023; accepted August 23, 2023

A physical model is formulated for the motion of liquid inclusions in a crystal in the field of forces caused by the presence of radiation point defects. The model is based on a statistical approach to the processes of induced transitions of structural elements of a crystalline matrix at the interfacial boundary with its solution. From the energy principle, an analytical dependence of the velocity of a spherical azimuthally symmetric inclusion on its size is obtained, considering the threshold nature of the motion. It is shown that the theoretical dependence correlates well with experimental results obtained for inclusions of aqueous saturated solution in potassium chloride crystals irradiated by high-energy electrons. The proposed model of the radiation-induced motion of a liquid inclusion is dynamic and allows us to interpret the nature of inclusion velocity changes in the crystal over time to determine the characteristic energy parameters of point defects.

Keywords: Crystal matrix; Point defects; Solution inclusion; Radiation-induced motion; Interfacial boundary; Statistical approach

PhySH: Surface & interfacial phenomena

The problem of radiation defect formation remains one of the most important topics in radiation damage physics and radiation materials science. Understanding the mechanisms of radiation defect formation in solids is necessary to increase the resistance of materials used in power generation or radioactive material storage, and to develop new materials (including nanostructured materials) with special properties that cannot be achieved by conventional synthesis methods (see [1] and references therein).

The problem of radiation defect formation also remains relevant for further improvement of technologies and methods for increasing the radiation resistance of semiconductor materials for various critical applications [2, 3], including the creation of X/γ-ray detectors (see [4, 5] and references in them).

At the same time, the problem of radiation defect formation has not been solved even for the simplest in-structure alkali halide crystals [6]. Although for more than a hundred years, alkali halide crystals, ionic systems with a simple electronic and crystal structure, have been model objects for studying radiation damage in materials caused by various types of radiation. It is known that irradiation of alkali metal halide crystals can produce Frenkel defect pairs in both the anionic and cationic sublattices. However, particular shockless formation mechanisms of Frenkel cation pairs (associated with the decay of various electronic excitations) remain unclear even today.

For many decades, alkali halide crystals have been topical objects not only for fundamental research but also for various applications. Optical media for recording and storing information, laser media, near-infrared light filters, thermoluminescent dosimeters, etc., have been proposed on their basis. [7]. One application of lithium fluoride, for example, is its use in the biological shielding of neutron-powered nuclear reactors. There are prospects for using lithium as an active element in thermonuclear fusion.

Our interest in the problem of the radiation defects formation and their subsequent dynamics during the thermal activation of alkali halide crystals in the medium temperature range (~300–600 K) is primarily due to the previously discovered effects of mass transfer on singular crystal faces modified by electron irradiation in vacuum [8] and in the process spontaneous migration of saturated solution inclusions in electron-irradiated water-soluble crystals (see [9] and references therein).

Study of surface mass transfer processes leading to elementary steps bunching is topical due to the need to obtain substrates for the production of low-dimensional structures (see [10–12] and references therein). And a study of motion and transformation of the shape of saturated solution inclusions in water-soluble crystals in the field of thermodynamic driving forces of various nature is of interest, in particular, for elucidating the mechanisms of crystallization under terrestrial conditions that exclude convective heat and mass transfer, which negatively affects the perfection of obtained crystals (see [13, 14] and references therein).

The purpose of this work is to construct a physical model of the motion of liquid inclusions in a crystal in the field of forces caused by the inhomogeneous distribution of radiation-induced point defects. As was shown earlier (see [9]

[†] **Cite as:** O.P. Kulyk, O.V. Podshyvalova, M.Yu. Shevchenko, V.I. Tkachenko, I.V. Hariachevska, T. Aoki, East Eur. J. Phys. 3, 570 (2023), <https://doi.org/10.26565/2312-4334-2023-3-67>

© O.P. Kulyk, O.V. Podshyvalova, M.Yu. Shevchenko, V.I. Tkachenko, I.V. Hariachevska, T. Aoki, 2023

and references therein), the presence of such thermodynamic nonequilibrium defects at a certain difference in their concentration can cause a chaotic inclusion motion at room temperatures under isothermal conditions. The presence of a dynamic model that adequately interprets the experimental data (including the time dependence of the inclusion velocity) may allow a better understanding of the radiation defect formation processes in alkali halide crystals.

PROBLEM STATEMENT

One of the experimentally detected features of the radiation-induced motion of liquid inclusions in crystals is the conservation of a rounded shape close to the equilibrium shape during their motion (see [9] and references therein).

Let us consider the case when the inclusion in the matrix has a spherical shape with a radius R_0 (see Fig. 1). To describe such an inclusion shape, a spherical coordinate system is introduced:

$$x = r \sin(\theta) \cos(\varphi), \quad y = r \sin(\theta) \sin(\varphi), \quad z = r \cos(\theta), \tag{1}$$

where $r = \sqrt{x^2 + y^2 + z^2}$, $\cos(\theta) = zr^{-1}$, $\text{tg}(\varphi) = yx^{-1}$, $0 \leq r < \infty, 0 \leq \theta \leq \pi, 0 \leq \varphi \leq 2\pi$.

For an azimuthal-symmetric inclusion, all unknown quantities do not depend on the angle φ , therefore one can assume $\varphi = 0$ anywhere. Variables r and θ remain independent. The gradient of inhomogeneity in the radiation defects density $\rho(\vec{r})$ (see Fig. 1) is directed at a polar angle $\theta = 0$. Thus, on opposite hemispheres of the inclusion, the radiation defect density differs by a small amount $\frac{\rho_2 - \rho_1}{\rho_2} \approx ((2\vec{R}_0)\vec{v}) \ll 1$, that is, the following inequality can be considered valid:

$$\frac{\rho_2 - \rho_1}{\rho_2} \approx \frac{((\vec{R}_0)\vec{v}) \rho_2}{\rho_2} \ll 1.$$

On the other hand, one assumes that the density of defects is so high that the distance between them is small compared to the size of the inclusion in the direction of the crystal inhomogeneity. This condition is equivalent to inequality $R_0 \sqrt[3]{\bar{\rho}} \gg 1$, where $\bar{\rho} = W_D^{-1} 2\pi \int_0^{\bar{R}} \int_0^\pi \rho(\vec{r}) r^2 dr \sin \theta d\theta$ is the average density of radiation defects in the crystal volume with radius $\bar{R} \gg R_0$.

Thus, to consider the macroscopic inclusion motion along the direction of radiation defect inhomogeneous distribution, the conditions have the following form:

$$(\sqrt[3]{\bar{\rho}})^{-1} \ll R_0 \ll \left(\frac{((\vec{R}_0)\vec{v}) \rho_2}{R_0 \rho_2} \right)^{-1}. \tag{2}$$

Figure 1 shows a schematic diagram of the inclusion in a crystal.

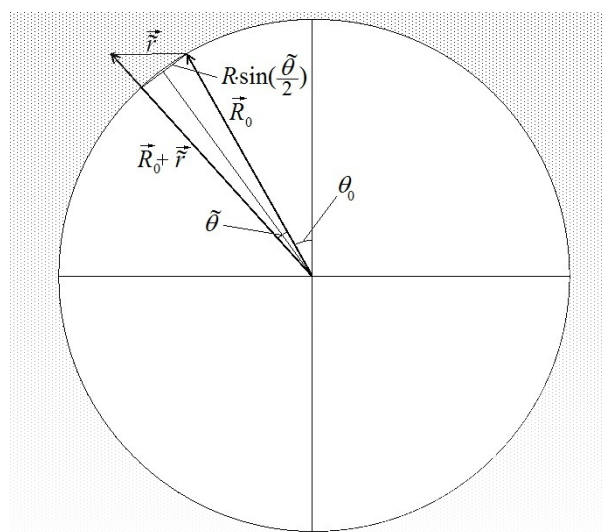


Figure. 1. Location diagram of a spherical azimuthally symmetric inclusion in a crystalline matrix.

The velocity of the spherical inclusion is assumed to be \vec{V}_0 . To simplify the calculations, let us move to the reference frame where the inclusion is at rest. Then the velocities of the crystal matrix and the radiation defects are given in the form $\vec{U}(R) = \vec{V}(R) - \vec{V}_0$, $|\vec{V}_0| \geq |\vec{V}(R)|$, where $\vec{V}(R) = \vec{V}(R_0 + (R - R_0)\vartheta(R - R_0))$ is the velocity of

the spherical inclusion of radius R , $\vec{V}(R_0) = \vec{V}_0$ is the inclusion velocity corresponding to the inclusion size threshold value R_0 , at which $\vec{U} = 0$. Here $\vartheta(x)$ is a unit function of the form $\vartheta(x < 0) = 0$; $\vartheta(x \geq 0) = 1$.

Thus, in the chosen reference frame, the crystal matrix with radiation defects either is at rest at $R \leq R_0$ or moves in the negative axis θ direction ($\theta = \pi$) when the inclusion size is larger than the critical: $R > R_0$.

In the new frame of reference the crystal matrix moves with a velocity $\vec{U}(R_0) = (U_r(R_0); U_\theta(R_0))$, where $U_r(R_0) = U_{r0} = \vec{U}(R_0)\vec{e}_r$, $U_\theta(R_0) = U_{\theta0} = \vec{U}(R_0)\vec{e}_\theta$, $\vec{e}_r, \vec{e}_\theta$ are unit vectors along the radial \vec{r} and polar θ axes, respectively.

The inclusion in the crystal contains a solvent that facilitates stress relaxation in the crystal due to accelerated diffusion and transfer of the matrix material in the solvent from the front hemisphere to the back. At that, the experimental fact of the inclusion motion without a significant change in its shape indicates the transition of matrix atoms into solution from the front inclusion surface, and an equal to it deposition of atoms from the solution onto the matrix on the back inclusion surface.

Such processes of matrix atom dissolution and crystallization are observed only in the field of forces of inhomogeneously stressed crystal, to which radiation defect inhomogeneous distribution can be referred. Therefore, the inhomogeneous distribution of point defects can be considered as a force that initiates inclusion displacement.

The processes of matrix atom transitions into solution and back have a probabilistic nature. Therefore, a two-level system can be used to describe such transitions.

STATISTICAL APPROACH

The processes occurring on the front and back surfaces of a spherical inclusion are similar to those observed when a crystal grows from a supersaturated solvent (vapor or liquid), or when it is dissolved in an unsaturated solvent [15-17]. Therefore, the previously developed models for describing such processes are also applicable to the description of the crystal inclusion motion, since they are based on the processes of crystal growth and dissolution.

The presence of a high defect density on the front inclusion surface makes the solvent unsaturated, and this surface dissolves. In turn, on the spherical inclusion back surface, where the defect density is lowered and the solvent is supersaturated, the growth is observed. Thus, the presence of a radiation defect density gradient causes the inclusion displacement in the direction of this gradient.

Let us consider a model that can explain the inclusion motion along the defect density gradient in a radiation-damaged crystal. In accordance with the above, the inclusion motion occurs in the direction of the axis θ . In this model, the following statistical approach is used to describe the process of inclusion motion in the matrix.

The elementary processes of the matrix atom transitions into solution and back on the front inclusion surface will be considered in the concept of a two-level system shown in Fig. 2.

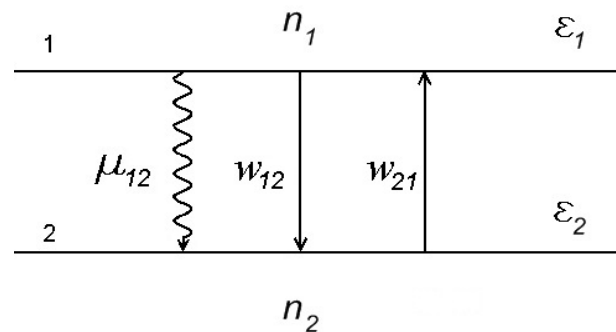


Figure 2. Scheme of a two-level system with populations n_1 and n_2 , energies ε_1 and ε_2 , transition probabilities: μ_{12} – spontaneous, w_{12} and w_{21} – induced

In Fig. 2, the arrows show the directions of atom transitions from one level to another: spontaneous transitions with probability μ_{12} , induced transitions with probabilities w_{12} and w_{21} . In Fig. 2, level 1 corresponds to the matrix atoms in the solvent, and level 2 corresponds to those held on the matrix surface.

In a stable crystal, when the difference in defect densities is less than the critical one, there is no inclusion motion. In this state, the difference between the free energies of an atom in the solvent and on the matrix surface is positive [18], i.e. $\varepsilon_1 > \varepsilon_2$.

Spontaneous transitions reduce the free energy of an atom in solution. Therefore, atoms spontaneously move from level 1 to level 2. The probability of spontaneous transitions μ_{12} determines the probability of a spontaneous transition of an atom in 1 second. Spontaneous transitions from the upper level to the lower level ($\varepsilon_1 \rightarrow \varepsilon_2$) are described by equations:

$$\frac{dn_1(t)}{dt} = -\mu_{12}n_1(t), \quad \frac{dn_2(t)}{dt} = \mu_{12}n_1(t), \quad (3)$$

where $n_{1,2}(t)$ are the populations of levels 1, 2 as functions of time t , μ_{12} is the probability of spontaneous transition. Since the inclusion displacement is observed only when the defect density difference on its front and back surfaces is higher than the critical one, it is assumed that the probability of the induced transition w_{im} also depends on the externally created difference between the point defect densities on the front and back inclusion surfaces. Then the probability of induced transitions can be represented as:

$$w_{im} = \alpha_{im}(\rho(z_0 + c) - \rho(z_0)) = \frac{\alpha_{im}\beta}{a^2} W = \bar{w}_{im}N, \tag{4}$$

where indices i, m take values 1, 2, ($i \neq m$), α_{im} are constant values, W is the inclusion volume, $\bar{w}_{im} = \frac{\alpha_{im}\beta}{a^2} W_0$ is the proportionality factor, W_0 is the characteristic volume of a solvent molecule, N is the number of solvent atoms (molecules) in the inclusion volume.

At the initial moment, the number of solvent atoms is denoted by the value $N(t)|_{t=0} \equiv N_0$, and it is assumed to be sufficiently large, i.e. $N_0 \gg n_{10}, n_{20}$, where $n_{10} = n_1(t)|_{t=0}$, $n_{20} = n_2(t)|_{t=0}$.

Consideration of induced processes caused by inhomogeneity of point defect density changes the form of the initial equations (4):

$$\frac{dn_1(t)}{dt} = -(\mu_{12} + \bar{w}_{12}N)n_1 + \bar{w}_{21}Nn_2, \quad \frac{dn_2(t)}{dt} = (\mu_{12} + \bar{w}_{12}N)n_1 - \bar{w}_{21}Nn_2. \tag{5}$$

Equation (6) should be supplemented by the equation for changing the solvent atom number $N(t)$, providing induced processes in the two-level system:

$$\frac{dN(t)}{dt} = -(\mu_{12} + \bar{w}_{12}N(t))n_1(t) + \bar{w}_{21}N(t)n_2(t). \tag{6}$$

From the condition of statistical equilibrium in a two-level system the Einstein relation follows $-\mu_{12} = \bar{w}_{12} = \bar{w}_{21}$ [19, 18]. This relation, for the case when induced processes dominate over spontaneous ones ($N_0 \gg n_{10}, n_{20}$), greatly simplifies the initial system of equations (5), (6):

$$\frac{dn_1(t)}{dt} = \mu_{12}(n_2(t) - n_1(t))N(t), \quad \frac{dn_2(t)}{dt} = -\mu_{12}(n_2(t) - n_1(t))N(t), \quad \frac{dN(t)}{dt} = -\mu_{12}(n_2(t) - n_1(t))N(t). \tag{7}$$

For spherically symmetric inclusions, the unknown quantities n_1, n_2, N, μ_{12} in equations (7) become dependent on the coordinates $R_0 + \tilde{r}, \theta_0 + \tilde{\theta}$, where \tilde{r} and $\tilde{\theta}$ correspond to a small ($|\tilde{r}| \ll R_0, |\tilde{\theta}| \ll |\theta_0|$) deviation of the radius and polar angle from R_0 and θ_0 , respectively.

Under these conditions, equations (7) are transformed to the form:

$$\begin{aligned} \frac{\partial n_1}{\partial t} + U_{r0} \frac{\partial n_1}{\partial \tilde{r}} + \frac{U_{\theta 0}}{R_0 + \tilde{r}} \frac{\partial n_1}{\partial \tilde{\theta}} &= \mu_{12}(n_2 - n_1)N, \\ \frac{\partial n_2}{\partial t} + U_{r0} \frac{\partial n_2}{\partial \tilde{r}} + \frac{U_{\theta 0}}{R_0 + \tilde{r}} \frac{\partial n_2}{\partial \tilde{\theta}} &= -\mu_{12}(n_2 - n_1)N, \\ \frac{\partial N}{\partial t} + U_{r0} \frac{\partial N}{\partial \tilde{r}} + \frac{U_{\theta 0}}{R_0 + \tilde{r}} \frac{\partial N}{\partial \tilde{\theta}} &= -\mu_{12}(n_2 - n_1)N, \end{aligned} \tag{8}$$

where $\mu_{12}(R_0 + \tilde{r}, \theta_0 + \tilde{\theta})$ is the function of \tilde{r} and $\tilde{\theta}$.

Let us find solutions to equations (8) in the simple case when the probability of induced transitions μ_{12} can be represented as an expansion in a Taylor series in small displacements \tilde{r} and $\tilde{\theta}$ [20]:

$$\mu_{12}(R_0 + \tilde{r}, \theta_0 + \tilde{\theta}) \approx \mu_{12}(R_0, \theta_0) \times \left(1 + \frac{1}{\mu_{12}(R_0, \theta_0)} \sum_{n=1}^{\infty} \frac{1}{n!} (\vec{\tilde{r}} \vec{\nabla})^n \mu_{12}(R_0, \theta_0) + \tilde{\theta} \lambda_{\theta} \right), \tag{9}$$

where $\vec{\tilde{r}} = \tilde{r} \cdot \vec{e}_r + \tilde{r}_{\theta} \cdot \vec{e}_{\theta}$, $\vec{\nabla} = \vec{e}_r \frac{\partial}{\partial \tilde{r}} + \vec{e}_{\theta} \frac{1}{R_0 + \tilde{r}} \frac{\partial}{\partial \tilde{\theta}}$, $\tilde{r}_{\theta} = R_0 \cdot 2 \sin\left(\frac{\tilde{\theta}}{2}\right) \approx R_0 \cdot \tilde{\theta}$ (see Fig. 1). Further, in the calculations, the sign " \sim " is omitted.

Consider the case when expansion (9) contains only odd powers r . Then expression (9) takes the form:

$$\mu_{12}(R_0 + r, \theta_0 + \theta) \approx \mu_{12}(R_0, \theta_0) \times \left(1 + \sum_{n=1}^2 \lambda_{r,2n-1} r^{2n-1} + \theta \lambda_{\theta} \right), \tag{10}$$

where $\lambda_{r,2n-1} = \frac{1}{\mu_{12}(R_0, \theta_0)} \frac{1}{(2n-1)!} \frac{\partial^{2n-1} \mu_{12}(R_0, \theta_0)}{\partial r^{2n-1}}$, $\lambda_\theta = \frac{1}{\mu_{12}(R_0, \theta_0)} \frac{\partial \mu_{12}(R_0, \theta_0)}{\partial \theta}$. Choosing such a power dependence of the induced transition probability on r under the condition $\lambda_{r,2n-1} > 0$ corresponds to the inclusion front surface, where the density of radiation defects increases with rising r . In this case, the matrix material dissolution is observed because the induced transition probability in the matrix is greater compared to the induced transition probability in the solution. This follows from the fact that the terms in (10) proportional to odd powers change sign, because in the solution $r < 0$.

On the back inclusion surface $\lambda_{r,2n-1} < 0$, and therefore the deposition of the dissolved crystal atoms on the matrix surface is observed, since the value of the probability of induced transitions in the matrix is less than in the solution.

Based on the type of expansion chosen in (10), a new variable is introduced $\xi(t, r, \theta) = t + \frac{r^2 \lambda_{r,1}}{2U_{r0}} + \frac{r^4 \lambda_{r,3}}{4U_{r0}} + \frac{R_0 \theta^2 \lambda_\theta}{2U_{\theta0}}$. Then equations (8) can be transformed to the form:

$$\frac{\partial n_1}{\partial \xi} = \mu(n_2 - n_1)N, \quad \frac{\partial n_2}{\partial \xi} = -\mu(n_2 - n_1)N, \quad \frac{\partial N}{\partial \xi} = -\mu(n_2 - n_1)N, \quad (11)$$

where, for simplification, the following notation is used $\mu = \mu_{12}(R_0, \theta_0)$.

The form of equation system (11) completely coincides with the form of equation system (7), with the only difference that the argument of system (11) is the function $\xi(r, \theta, t)$. Therefore, the solutions of system (11) coincide with the solutions of (7), where argument t must be replaced by argument $\xi(r, \theta, t)$, and μ_{12} must be replaced by μ .

VELOCITY OF THE SPHERICAL AZIMUTHAL-SYMMETRIC INCLUSION

To determine the inclusion velocity V , the plane of constant phase is set. This plane is defined by:

$$\xi(t, r, \theta) = D \quad (12)$$

where D is the constant.

It follows from equation (12) that for a given time $t = t_R$ and $D = D_R$ it is possible to construct a second-order azimuthal-symmetric surface, which determines the dependence of its radial coordinate on r the polar angle θ .

If one fixes $D = D_R$, then over time the azimuthal-symmetric surface of the second order moves in space together with the matrix with a velocity of U_R . This velocity is determined from the expression for the total time derivative of the equation (12):

$$1 + \frac{r \lambda_{r,1}}{U_{r0}} U_R + \frac{r^3 \lambda_{r,3}}{U_{r0}} U_R + \frac{R_0 \theta \lambda_\theta}{U_{\theta0}} \frac{1}{r} U_\theta = 0, \quad (13)$$

where $U_R = \frac{dr}{dt}$ is the radial velocity of a constant phase surface, $U_\theta = r \frac{d\theta}{dt}$ is the polar velocity of a constant phase surface.

The angular velocity of the constant phase surface is expressed in terms of the surface radial velocity, based on the following considerations. Since the matrix moves as a whole, and the spherical inclusion is at rest and does not change its shape, the polar velocity U_θ of a point on its surface at $\theta = \frac{\pi}{2}$ is equal to the radial velocity of a point on its surface at $\theta = 0$, i.e. $U_\theta = U_R$.

On this basis, it follows from (13):

$$U_R = -\frac{Ax}{B+x^2+Cx^4} \quad (14)$$

where $x = \frac{r}{R_0}$, $A = \frac{U_{r0}}{R_0 \lambda_{r,1}}$, $B = \frac{\pi U_{r0} \lambda_\theta}{2 U_{\theta0} R_0 \lambda_{r,1}}$, $C = \frac{R_0^2 \lambda_{r,3}}{\lambda_{r,1}}$.

Assuming $r = R$ in (14), the dependence of the matrix velocity on the spherical inclusion radius is obtained:

$$U_R = -\frac{Ax_R}{B+x_R^2+Cx_R^4}, \quad (15)$$

where $x_R = R/R_0$.

Expression (15) determines the matrix velocity in the frame of reference where the inclusion is at rest. In the laboratory frame of reference, where the matrix is at rest, the inclusion velocity has the opposite sign:

$$U'_R = \frac{Ax_R}{B+x_R^2+Cx_R^4}, \quad (16)$$

where the sign "-" already determines the inclusion velocity. Further, the sign "-" is omitted.

Since the inclusion motion is observed only at radii exceeding the threshold value of the inclusion radius R_0 , it is possible to replace $x_R \rightarrow x_R - 1$ in (16), which corresponds to the transition to the calculation of velocity dependence not on the inclusion radius R , but on its exceeding the threshold value.

Thus, taking into account the above replacement and equation (16), it follows that for small inclusion radii, when $|x_R - 1| \ll 1$ and $A > 0, B > 0$, its velocity linearly increases as $V_R \approx V_0 + \frac{A}{B}(x_R - 1)$ with increasing inclusion radius. As the inclusion radius increases, the velocity reaches a maximum value and then, at $|x_R - 1| \gg 1$, decreases as $V_R \approx V_0 + \frac{A}{Cx_R^3}$, where $A > 0, C > 0$.

ENERGY INTERPRETATION OF THE INCLUSION VELOCITY

The spherical inclusion velocity U_R can be related to the matrix velocity U_{r0} using the energy relations.

The flow of point radiation defects with density $\rho(z)$ creates a "wind" moving at speed $U_R = U_{r0}$. The wind pressure force of radiation defects on the inclusion is equal to the difference in pressure forces on its front and back hemispheres with an area of the order of $S = \pi R_0^2$:

$$F_D = C_w \frac{1}{2} (\rho_2 - \rho_1) m_D S U_{r0}^2 = C_w \frac{1}{2} \beta m_D W U_{r0}^2, \quad (17)$$

where m_D is the effective mass of a point defect, $W = \pi R_0^3$ is the volume of the order of inclusion volume, C_w is the dimensionless resistance coefficient, $\beta = \frac{\rho_2 - \rho_1}{R_0}$ is the density gradient of radiation defects, ρ_2, ρ_1 are the radiation defect densities at the front and back poles of the spherical inclusion, respectively.

If the inclusion moves with velocity V' in the direction of the force (17), its velocity U_R is lower, and therefore the pressure force decreases:

$$F'_D = C_w \frac{1}{2} \beta m_D W (U_{r0} - V')^2. \quad (18)$$

The power produced by the pressure force (17) is equal to:

$$P_D = C_w \frac{1}{2} \beta m_D W (U_{r0} - V')^2 V'. \quad (19)$$

It follows from (19) that the maximum power is achieved at $V' = \frac{U_{r0}}{3}$ [21], and is equal to:

$$P_D^{max} = \frac{4}{27} C_w \frac{1}{2} \beta m_D W U_{r0}^3. \quad (20)$$

The maximum power (20) is chosen based on the principle of least action, which determines the way of optimal stress relief in the crystal: the radiation stress of the crystal must be reset in the minimum time. The maximum power of the inclusion motion corresponds to the minimum time of stress relaxation in the crystal.

Thus, expression (20) determines the maximum power, which the inclusion gains by the wind of radiation defects blowing over it.

On the other hand, this power is spent on overcoming the resistance force F_R , which opposes the inclusion motion. The power expended to move an inclusion over a distance $r(t + \Delta t) - r(t)$ in little time Δt is determined by the following expression:

$$P_R = F_R \lim_{\Delta t \rightarrow 0} \left(\frac{r(t + \Delta t) - r(t)}{\Delta t} \right) = F_R \left. \frac{dr}{dt} \right|_{\Delta t \rightarrow 0} = F_R \frac{Ax}{B + x^2 + Cx^4}, \quad (21)$$

where $F_R = \kappa(U_{r0} - V') = \frac{2}{3} \kappa U_{r0}$ is the resistance force created by the inhomogeneity of the radiation defect density distribution and κ is the coefficient of proportionality.

From the equality $P_D = P_R$, the velocity of inclusion motion U_{r0} is defined, assuming that the coordinate r is equal to the coordinate of the front inclusion face $r = R_0$:

$$V = V_0 + F(x_R), \quad (22)$$

where $F(x_R) = \frac{\delta x_R}{B + x_R^2 + Cx_R^4}$, $\delta = \frac{4}{3} \frac{\kappa}{\beta m_D W R_0 \lambda_{r,1}}$.

To determine the parameters V_0, A, B, C in (22), the experimental data [22] are used.

In Fig. 3, the solid line corresponds to the graph constructed using the analytical expression (22) and experimental data are shown with a marker \circ .

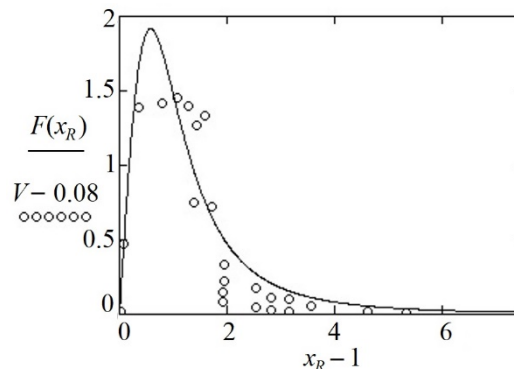


Figure 3. Dependence of the inclusion velocity on its longitudinal size (markers \circ correspond to experimental points), $V_0 = 0.08 \cdot 10^{-10}$ m/s [22], $\delta = 2.8$, $B = 0.5$, $C = 0.5$.

Comparison of theoretical calculations with experimental data indicates an adequate description of the experiment by the proposed theoretical model.

CONCLUSIONS

In the present work, a physical model of the liquid inclusion motion in the field of forces due to the inhomogeneous distribution of radiation point defects has been developed based on the statistical approach to the processes of induced transitions of matrix atoms into solution and back. The analytical dependence of the velocity of a spherical azimuthally symmetric inclusion on its size is obtained from the energy principle. It is shown that the analytical expression for the inclusion velocity describes the experimental results quite well. The proposed model of radiation-induced inclusion motion can be used to estimate the characteristic energy parameters of point defects inhomogeneously distributed in a crystalline medium.

Acknowledgements

This research was partly supported by the 2023 (grants 2074 and 2076) Cooperative Research Projects at Research Institute of Electronics, Shizuoka University, Japan.

ORCID

Oleksandr P. Kulyk, <https://orcid.org/0000-0002-7389-3888>;
 Oksana V. Podshyvalova, <https://orcid.org/0000-0001-9680-9610>
 Victor I. Tkachenko, <https://orcid.org/0000-0002-1108-5842>;
 Iryna V. Hariachevska, <https://orcid.org/0000-0002-4630-9519>
 Toru Aoki, <https://orcid.org/0000-0002-6107-3962>;
 Mykhailo Yu. Shevchenko, <https://orcid.org/0009-0007-5811-0113>

REFERENCES

- [1] N.A. Azarenkov, V.N. Vojevodin, V.G. Kirichenko, G.P. Kovtun, The Journal of Kharkiv National University, Physical series "Nucleus, Particles, Fields". 1(45) 887, 4 (2010), [http://nuclear.univer.kharkov.ua/lib/887_1\(45\)_10_p04-24.pdf](http://nuclear.univer.kharkov.ua/lib/887_1(45)_10_p04-24.pdf)
- [2] L.I. Barabash, I.N. Vishnevsky, A.A. Groza, A.Ya. Karpenko, P.G. Litovchenko, M.I. Starchik, Problems of Atomic Science and Technology. 2, 182 (2007), <https://vant.kipt.kharkov.ua/TABFRAME2.html>
- [3] A. Karmakar, J. Wang, J. Prinzie, V. Smedt, P. Leroux, Radiation. 1(3), 194 (2021), <https://doi.org/10.3390/radiation1030018>
- [4] V. Gnatyuk, O. Maslyanchuk, O. Kulyk, S. Shishiyanu, T. Aoki, Proceedings of SPIE, 12241, 122410M-1-8 (2022), <https://doi.org/10.1117/12.2633410>
- [5] V. Gnatyuk, S. Levytskyi, O. Maslyanchuk, O. Kulyk, T. Aoki, Proceedings of SPIE, 12126, 1212614-1-8 (2021), <https://doi.org/10.1117/12.2615569>
- [6] A. Lushchik, Ch. Lushchik, E. Vasil'chenko, A.I. Popov, Low Temperature Physics/Fizika Nizkikh Temperatur, 44(4), 357 (2018), <https://doi.org/10.1063/1.5030448>
- [7] N. Itoh, A.M. Stoneham, *Materials Modification by Electronic Excitation*, (Cambridge University Press, 2000), 520 p.
- [8] O.P. Kulyk, O.V. Podshyvalova, Bulletin of Kharkiv National Automobile and Highway University, 36, 91 (2007). (In Russian).
- [9] A.P. Kulik, O.V. Podshyvalova, and I.G. Marchenko, Problems of Atomic Science and Technology, 2(120), 13 (2019), https://vant.kipt.kharkov.ua/ARTICLE/VANT_2019_2/article_2019_2_13.pdf
- [10] O.P. Kulyk, V.I. Tkachenko, O.V. Podshyvalova, V.A. Gnatyuk, and T. Aoki, J. Cryst. Growth, 530, 125296-1-7 (2020), <https://doi.org/10.1016/j.jcrysgro.2019.125296>
- [11] O.L. Andrieieva, V.I. Tkachenko, O.P. Kulyk, O.V. Podshyvalova, V.A. Gnatyuk, T. Aoki, East European Journal of Physics, 4, 59 (2021), DOI: 10.26565/2312-4334-2021-4-06
- [12] O.P. Kulyk, O.V. Podshyvalova, O.L. Andrieieva, V.I. Tkachenko, V.A. Gnatyuk, T. Aoki, Problems of Atomic Science and Technology, 1(137), 154 (2022), <https://doi.org/10.46813/2022-137-154>
- [13] O.P. Kulyk, L.A. Bulavin, S.F. Skoromnaya, and V.I. Tkachenko, in: *Engineering for Sustainable Future. Inter-Academia 2019. Lecture Notes in Networks and Systems(LNNS)*, vol. 101, edited by A.R. Varkonyi-Koczy (Springer, Cham, 2020) pp. 326-339, https://doi.org/10.1007/978-3-030-36841-8_32

- [14] O.P. Kulyk, V.I. Tkachenko, O.L. Andrieieva, O.V. Podshyvalova, V.A. Gnatyuk, T. Aoki, in: *Research and Education: Traditions and Innovations. INTER-ACADEMIA 2021. Lecture Notes in Networks and Systems*, vol. 422 (Springer, Singapore, 2022) pp. 141-158, https://doi.org/10.1007/978-981-19-0379-3_14
- [15] Ya.E. Geguzin, and N.N. Ovcharenko, *Sov. Phys. Uspekhi*, **5**(1), 129 (1962), <https://dx.doi.org/10.1070/PU1962v005n01ABEH003403>
- [16] W.W. Mullins, *Journal of Applied Physics*, **30**(1), 77 (1959), <https://doi.org/10.1063/1.1734979>
- [17] Ya.E. Geguzin, Yu.S. Kaganovskij. *Diffusion Processes on a Crystal Surface*, (Ehnergoatomizdat, Moscow,1984), 128 p. (In Russian).
- [18] V.M. Kuklin, *The Journal of Kharkov National University, Physical series: Nuclei, Particles, Fields*, **933**(4/48), 4 (2010). (In Russian).
- [19] A. Einstein, *Physikalische Gesellschaft Zürich, Mitteilungen* **18**, 47 (1916).
- [20] H.B. Dwight, *Tables of Integrals and Other Mathematical Data*, 4th edition, (The Macmillan Company, 1961).
- [21] A. Betz, *Die Naturwissenschaften*, **XV**(46) 905 (1927).
- [22] V.S. Kruzhanov, O.V. Podshyvalova, *Sov. Solid State Physics*, **32**(2) 373 (1990). (In Russian).

МОДЕЛЬ РАДІАЦІЙНО-ІНДУКОВАНОГО РУХУ РІДКИХ ВКЛЮЧЕНЬ У КРИСТАЛІ

Олександр П. Кулик^a, Оксана В. Подшивалова^b, Михайло Ю. Шевченко^{a,c},

Віктор І. Ткаченко^{a,c}, Ірина В. Гарячевська^a, Тору Аокі^d

^aХарківський національний університет імені В.Н. Каразіна, Харків, Україна

^bНаціональний аерокосмічний університет "Харківський авіаційний інститут", Харків, Україна

^cІНЦ "Харківський фізико-технічний інститут" НАН України, Харків, Україна

^dНауково-дослідний інститут електроніки, Університет Шизуоки, Хамамацу, Японія

Сформульовано фізичну модель руху рідких включень у кристалі у полі сил, спричинених наявністю точкових дефектів радіаційного походження. В основу моделі покладено статистичний підхід до процесів індукованих переходів структурних елементів кристалічної матриці на міжфазній границі з власним розчином. З енергетичного принципу отримано аналітичну залежність швидкості сферичного азимутально-симетричного включення від його розміру, що враховує пороговий характер руху. Показано, що теоретична залежність добре корелює з експериментальними результатами, отриманими для включень насиченого водного розчину в кристалах хлориду калію, опромінених високоенергетичними електронами. Запропонована модель радіаційно-індукованого руху рідкого включення є динамічною і дозволяє інтерпретувати характер зміни швидкостей включень у кристалі у часі для визначення характерних енергетичних параметрів точкових дефектів.

Ключові слова: кристалічна матриця; точкові дефекти; включення розчину; радіаційно-індукований рух; міжфазна межа; статистичний підхід